



DAFA meeting

07/01/2025

Funded by
the European Union



**Barcelona
Supercomputing
Center**
Centro Nacional de Supercomputación



EXCELENCIA
SEVERO
OCHOA

Lightweight methods for Satellite-based emission estimation over Canary Islands and USA power plants

Andrés Yarce Botero, Emanuele Emili, Jeronimo Escribano, Guillaume Monteil, and Marc Guevara

Atmospheric Composition group, Earth Science department.
Data Assimilation Forecasting and Applications (AC-DAFA) Emissions (AC-EMIS)



GOBIERNO
DE ESPAÑA

VICEPRESIDENCIA
TERCERA DEL GOBIERNO
MINISTERIO
PARA LA TRANSICIÓN ECOLÓGICA
Y EL RETO DEMOGRÁFICO



Plan de Recuperación,
Transformación
y Resiliencia

AEMet
Agencia Estatal de Meteorología

BSC
Supercomputing
Center
Centro Nacional de Supercomputación

Outline

- Introduction
- Emission estimation problem and Satellite information for monitoring the atmospheric composition.
- Mathematical description of the Lightweight methods for satellite emission estimation (**Gauss Plume (GP)**, **Cross Sectional Flux (CSF)**, **Integrate Mass Enhancement (IME)**, Flux Divergence method (FD))
- The Canary Islands and EEUU case.
- Early conclusions.
- References.

Emission estimation problem

Emission inventories

Bottom-Up

Activity-Based Calculations: activity \times emission factor

Direct Measurements

Equipment/Process-Based Estimation

Surveys and Questionnaires

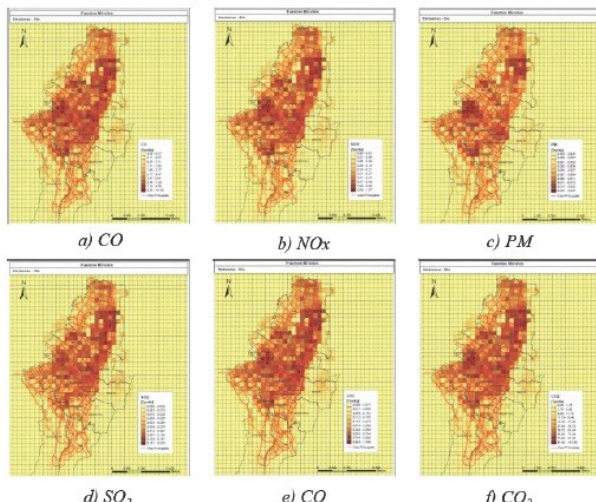
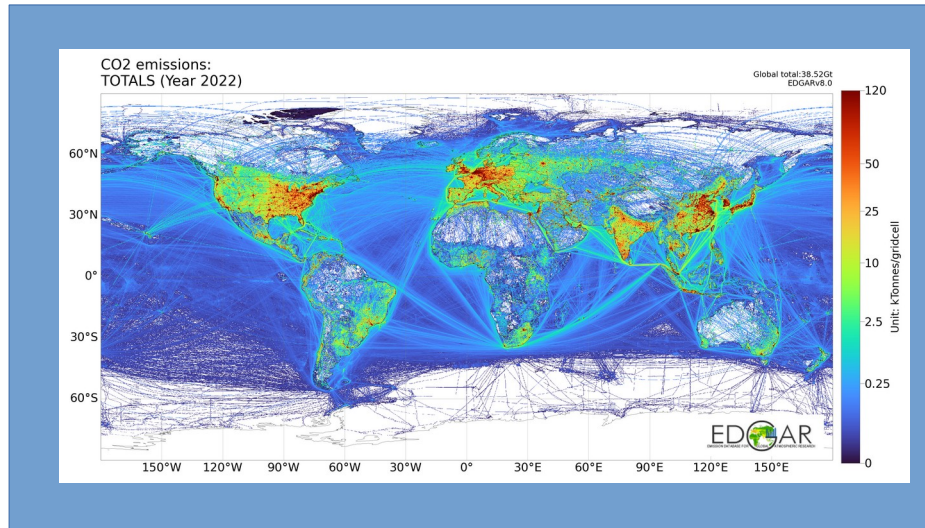


Figura 5. Desagregación espaciotemporal para fuentes móviles para 24 horas en día hábil

**



Hybrid Approaches

Data Fusion

Spatial Disaggregation

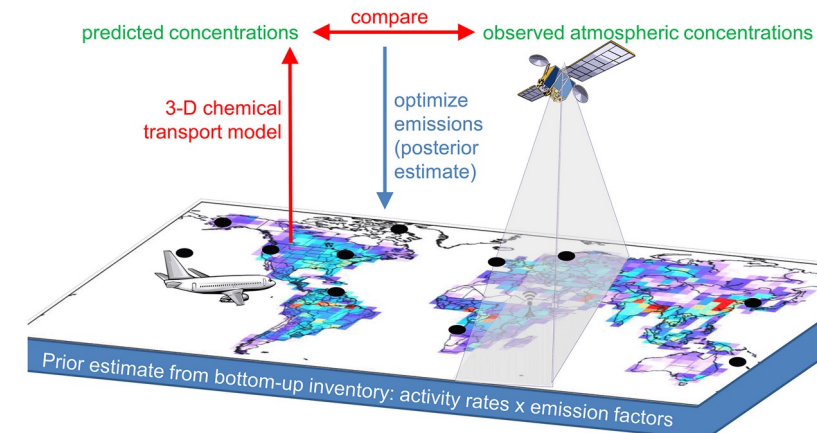
Top-Down

Energy Balance Approaches

Inverse Modeling

Proxy Data Scaling

Using atmospheric methane observations to test emission inventories

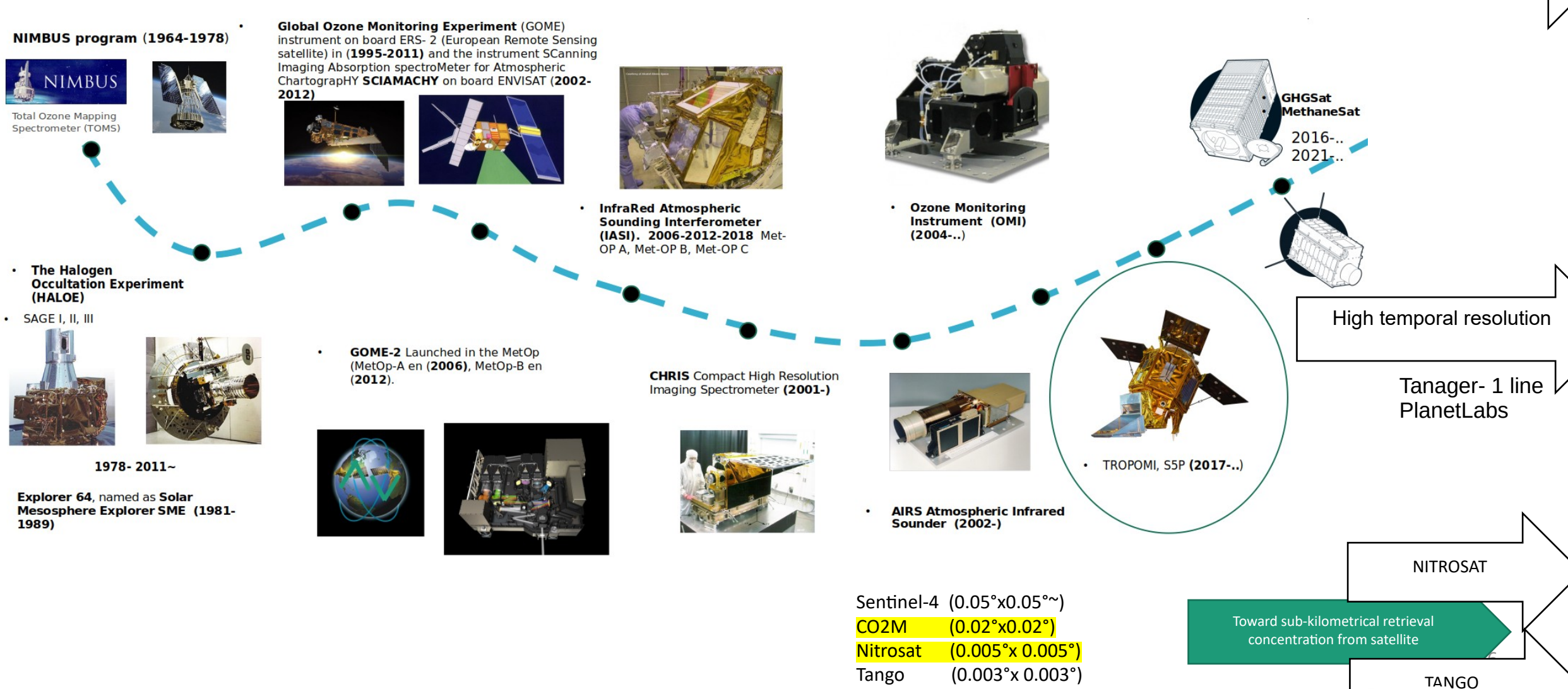


* Worden, J. R., Cusworth, D. H., Qu, Z., Yin, Y., Zhang, Y., Bloom, A. A., ... & Jacob, D. J. (2022). The 2019 methane budget and uncertainties at 1° resolution and each country through Bayesian integration Of GOSAT total column methane data and a priori inventory estimates. *Atmospheric Chemistry and Physics*, 22(10), 6811-6841.

** Carmona Aparicio, L. G., Rincón Pérez, M. A., Castillo Robles, A. M., Galvis Remolina, B. R., Sáenz Pulido, H. E., & Pachón Quinche, J. E. (2016). Conciliación de inventarios top-down y bottom-up de emisiones de fuentes móviles en Bogotá, Colombia. *Tecnura*, 20(49), 59-74.

Satellite information for monitoring the atmospheric composition

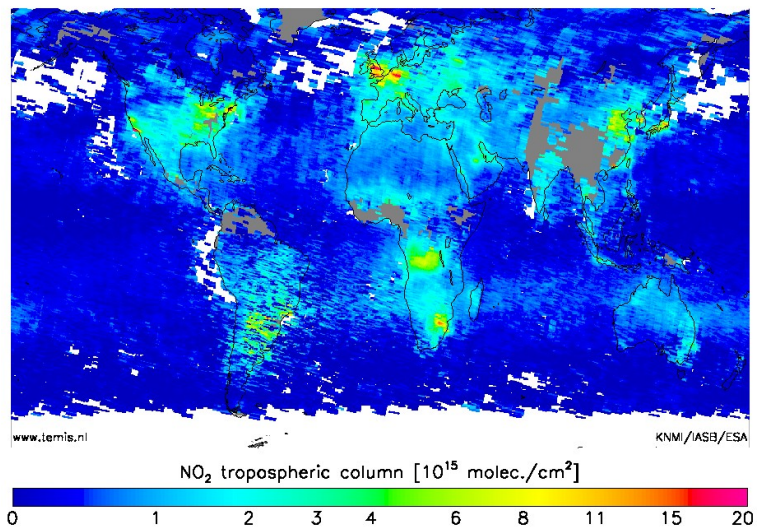
Orbital Spectrometer Timeline and near future prospects



Satellite instruments dedicated to atmospheric composition study

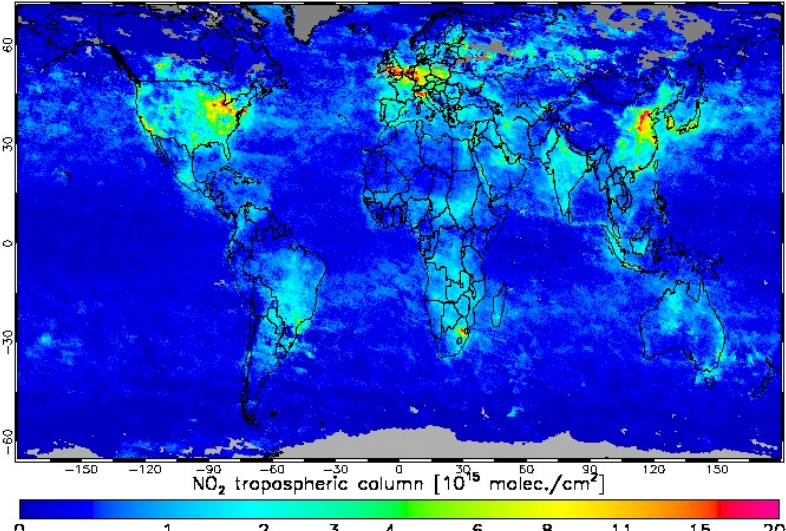
GOME tropospheric NO₂ July 1996

KNMI/IASB/ESA



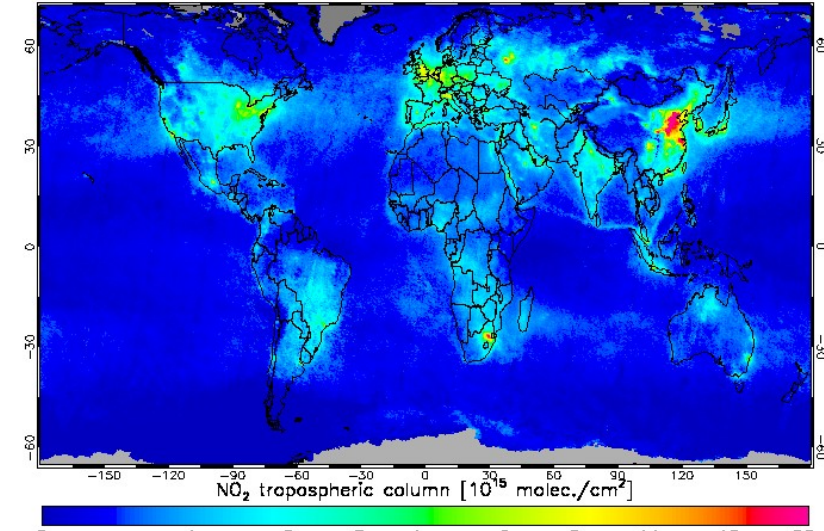
SCIAMACHY trop. NO₂ Oct. 2002

QA4ECV



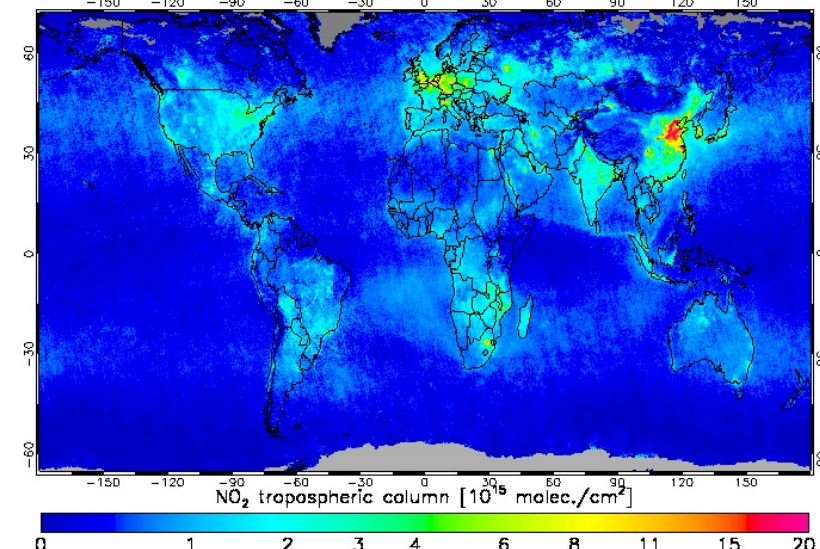
GOME2-A trop. NO₂ Oct. 2007

QA4ECV



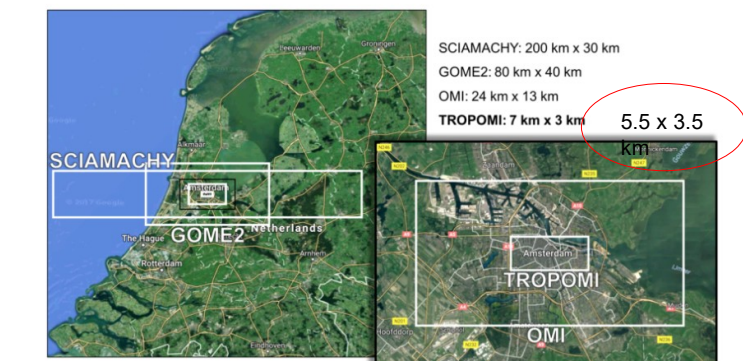
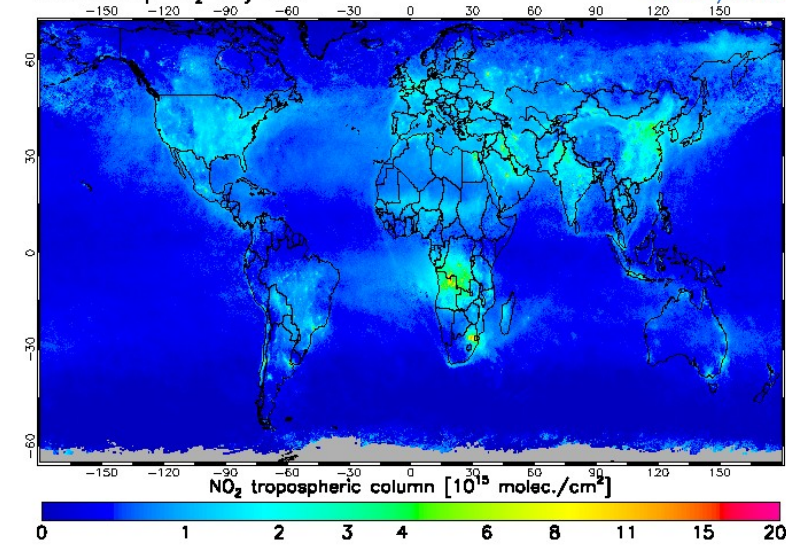
OMI trop. NO₂ Oct. 2015

QA4ECV



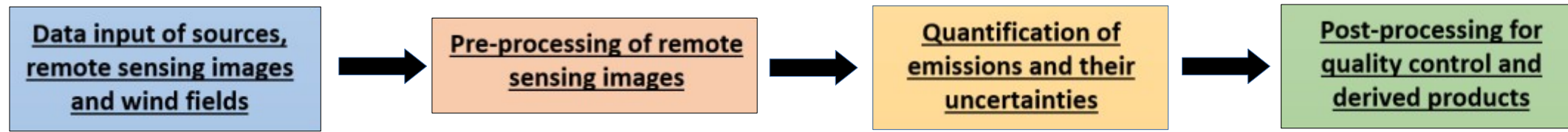
TROPOMI trop. NO₂ July 2024

KNMI/ESA



Lightweight emission estimation methods

Ddeq (Data driven emission quantification) v 1.0



Kuhlmann, G., Koene, E., Meier, S., Santaren, D., Broquet, G., Chevallier, F., ... & Brunner, D. (2024). The **ddeq** Python library for point source quantification from remote sensing images (version 1.0). *Geoscientific Model Development*, 17(12), 4773-4789.



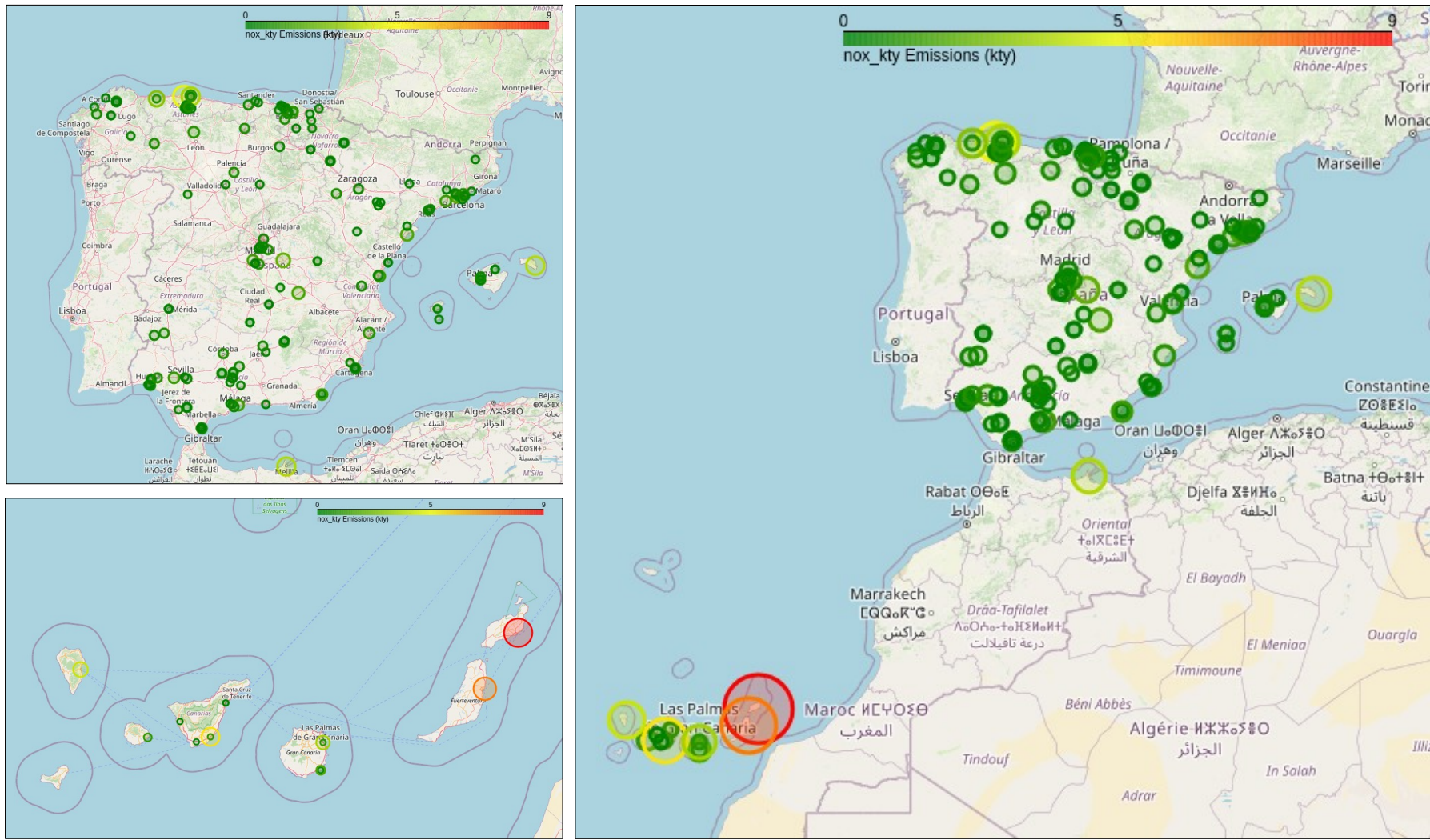
Funded by
the European Union



Plan de Recuperación,
Transformación
y Resiliencia

AEMet
Agencia Estatal de Meteorología

BSC
Barcelona
Supercomputing
Center
Centro Nacional de Supercomputación



Power Plants in Spain from CORSO V4 emission inventory

Plant Name	Sector	Fuel	Longitude	Latitude	CO2 (kty)	CH4 (kty)	NOx (kty)	SOx (kty)	CO (kty)
CENTRAL DIESEL LOS GUINCHOS	Power	Oil	-17.768000	28.665000	158.000000	0.014150	3.580000	0.586000	0.040921
CENTRAL DIESEL EL PALMAR	Power	Oil	-17.115031	28.087770	1096.153912	0.098171	0.842000	0.815999	0.283895
CONJUNTO DE TURBINA DE GAS DE GUÍA DE ISORA	Power	Oil	-16.803795	28.222538	11.143278	0.000432	0.008840	0.000151	0.002160
TURBINA DE GAS DE ARONA	Power	Oil	-16.642941	28.049548	25.079612	0.000972	0.020970	0.008980	0.004860
CENTRAL TÉRMICA DE GRANADILLA	Power	Oil	-16.509191	28.090942	1739.972415	0.155832	5.019962	0.932000	0.501516
CENTRAL TÉRMICA DE GRANADILLA	Power	Gas	-16.509191	28.090942	0.027585	0.000002	0.000038	0.000000	0.000009
CENTRAL TÉRMICA DE CANDELARIA	Power	Gas	-16.357656	28.381697	0.000592	0.000000	0.000000	0.000000	0.000000
CENTRAL TÉRMICA DE CANDELARIA	Power	Oil	-16.357656	28.381697	35.443577	0.001374	0.028554	0.010616	0.006869
CENTRAL TÉRMICA BARRANCO DE TIRAJANA	Power	Oil	-15.435877	27.804006	1579.981355	0.141503	1.309993	0.527000	0.409203
CENTRAL TÉRMICA BARRANCO DE TIRAJANA	Power	Gas	-15.435877	27.804006	0.018645	0.000002	0.000007	0.000000	0.000004
CENTRAL TÉRMICA JINÁMAR	Power	Coal	-15.411372	28.042431	51.614797	0.000782	0.136444	0.020567	0.009830
CENTRAL TÉRMICA JINÁMAR	Power	Oil	-15.411372	28.042431	134.385203	0.015881	2.933556	0.393433	0.038519
CENTRAL DIESEL LAS SALINAS	Power	Oil	-13.844870	28.504303	377.039556	0.033768	6.880000	0.988000	0.097650
CENTRAL DIESEL DE PUNTA GRANDE	Power	Oil	-13.516516	28.978510	432.000000	0.038690	9.020000	1.400000	0.625000

For the analysis we took the power plants that from the CORSO inventory exceed 3.0 (Kty)



LOS GUINCHOS



Photo by
Marc Ryckaert
(MJR) 22 December 2013. Creative Commons [Attribution 3.0 Unported](#) license.

PUNTA PIEDRA



Photo from Manolo de la Hoz (CC-BY-SA)

LAS SALINAS



Photo from [Andy Mitchell](#) from Glasgow, UK (CC-BY-SA)

GRANADILLA



Photo by
Jose Mesa, 24 January 2009. [Creative Commons Attribution 2.0 Generic](#) license.



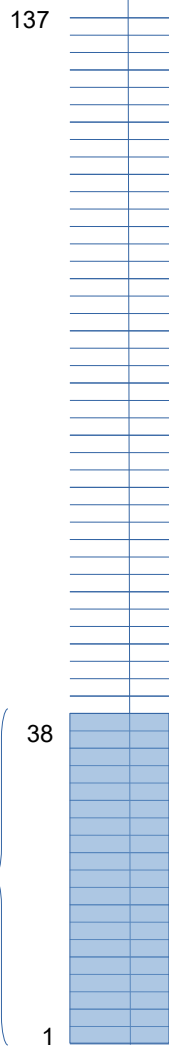
JINAMAR



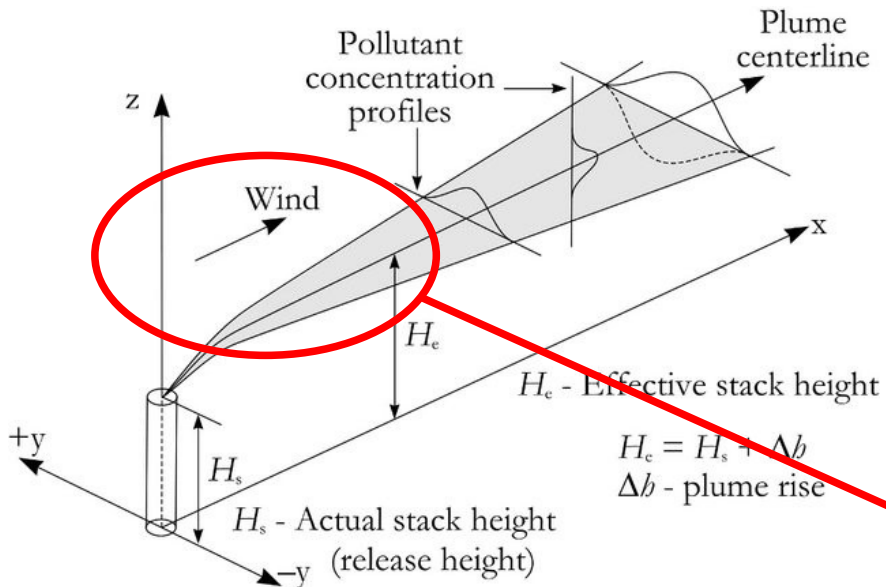
Photo by Erlend Bjørkvedt (CC-BY-SA)

Effective winds at the emission estimation location

ERA 5 Global reanalysis product levels used

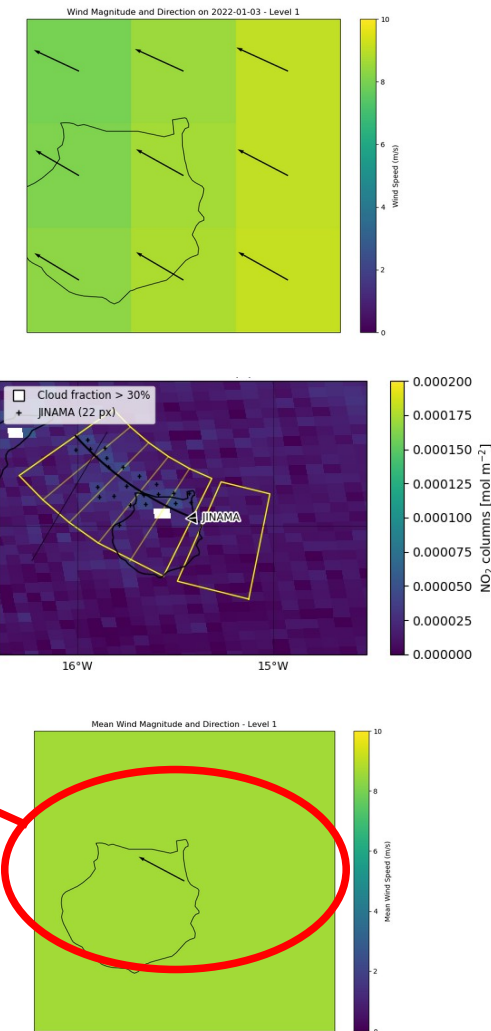


ERA 5 Global reanalysis product



$$H_e = H_s + \Delta b$$

Δb - plume rise

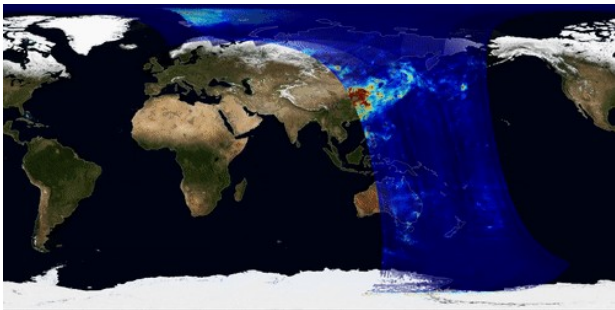


The effective stack height depends on the **temperature, emission velocity, diameter of the stack, humidity, wind speed and atmospheric stability**

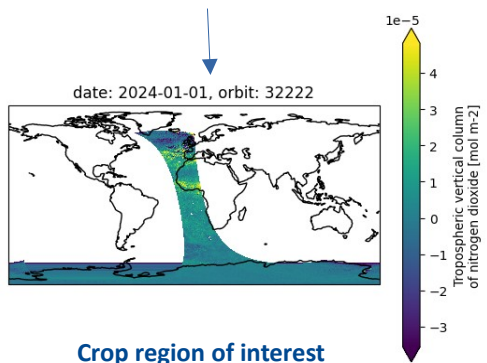
Plume model image from Leelössy, Á., Molnár, F., Izsák, F., Havasi, Á., Lagzi, I., & Mészáros, R. (2014). Dispersion modeling of air pollutants in the atmosphere: a review. Open Geosciences, 6(3), 257-278.

Preprocessing: Orbit selection based on point source and plume detection

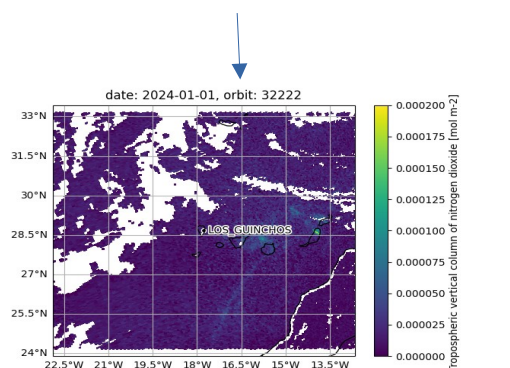
* GIF from: <https://www.aeronome.be/en/news/2021/three-years-tropomi-measurements>



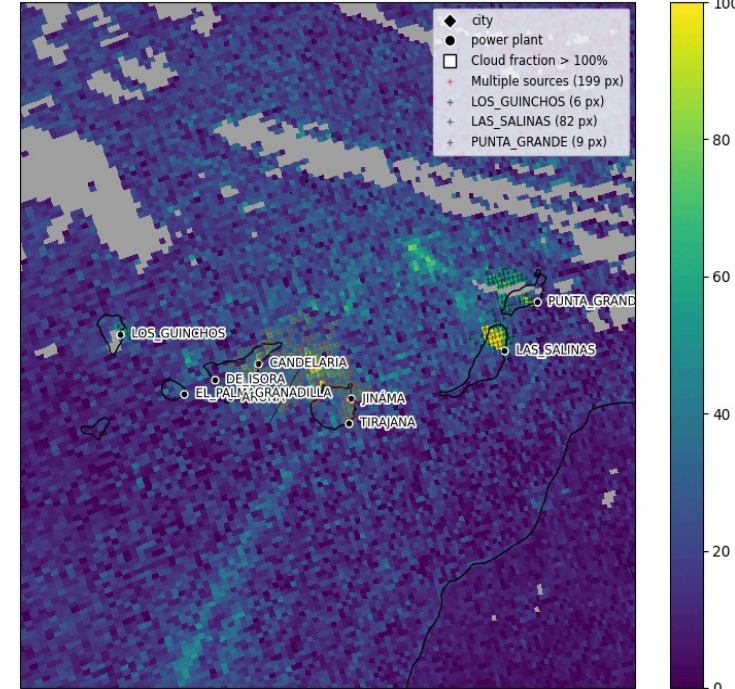
Metadata filtering to download specific orbit



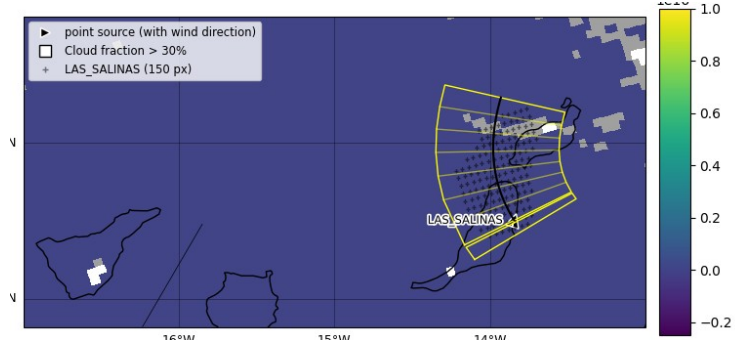
Crop region of interest



Orbit selection



Plume detection



Plume georeference system

$$SNR = \frac{X - X_{bg}}{\sqrt{\sigma_{\text{random}}^2 + \sigma_{\text{sys}}^2}} \geq z_{\text{thr}}$$

The threshold z_{thr} is computed from the probability (q) that the **local mean** is larger than the background given the uncertainty σ_{ov} based on a statistical **z test**.

The **local mean** is computed by applying a uniform or a Gaussian filter to the image

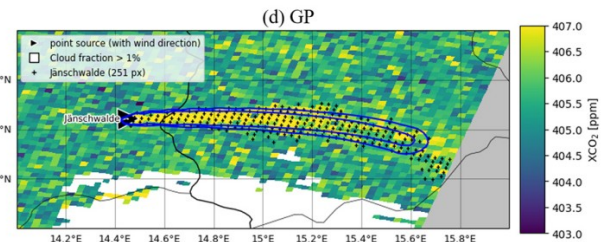
Emission estimation

Gaussian Plume

$$G(x, y) = \frac{Q H(x)}{\sqrt{2\pi} u \sigma(x)} \exp\left(-\frac{y^2}{2\sigma(x)^2}\right) + V_{\text{bg}}(x, y)$$

$$J(Q, K, V_{\text{bg}}, \kappa) = \|V_{i,j} - G(x_i, y_i)\|_2^2,$$

↓
Emission rate



Integrate Mass Enhancement

$$M = \int_{y_1}^{y_2} \int_{x_1}^{x_2} (G(x, y) - V_{\text{bg}}(x, y)) \, dx \, dy$$

$$M = \sum_{(i,j) \in \mathcal{P}_a} (V_{i,j} - V_{\text{bg}}) \cdot A_{i,j}$$

$$M = \int_{x_1}^{x_2} \frac{Q}{u} \, dx$$

$$\bar{Q} = \frac{u}{L} M$$



**Barcelona
Supercomputing
Center**
Centro Nacional de Supercomputación

Lightweight emission estimation methods

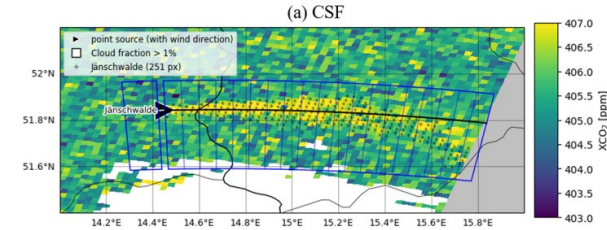
Cross Sectional Flux

$$F = u \cdot q$$

$$q(x) = \int_{y_1}^{y_2} (V(x, y) - V_{\text{bg}}) \, dy$$

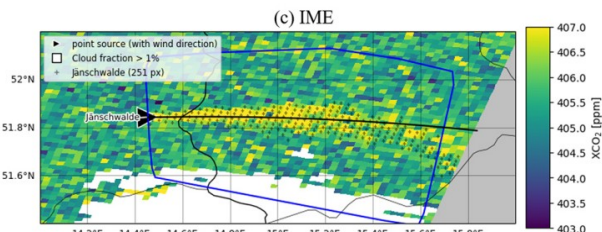
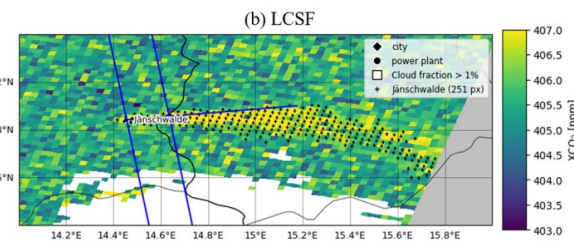
$$g(y) = \frac{q}{\sqrt{2\pi}\sigma} \exp\left(-\frac{(y-\mu)^2}{2\sigma^2}\right) + my + b,$$

$$\bar{Q} = \frac{F(x)}{D(x, \tau)}$$



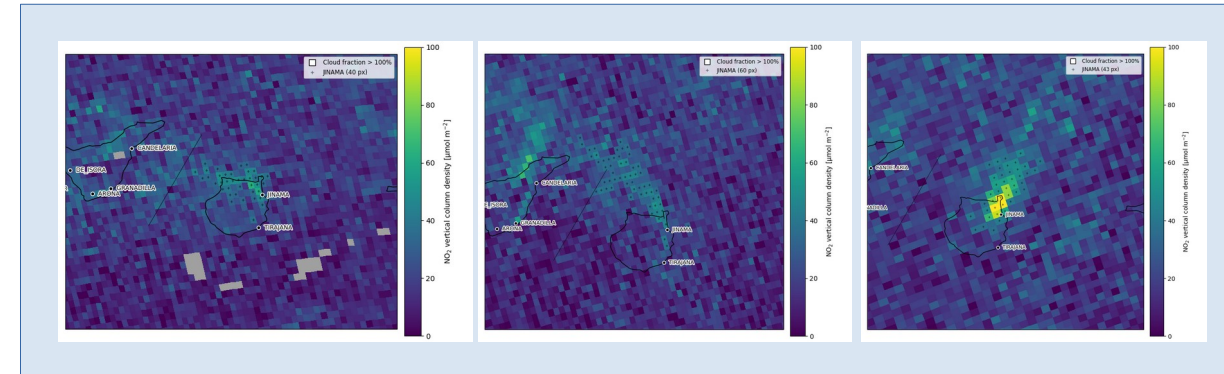
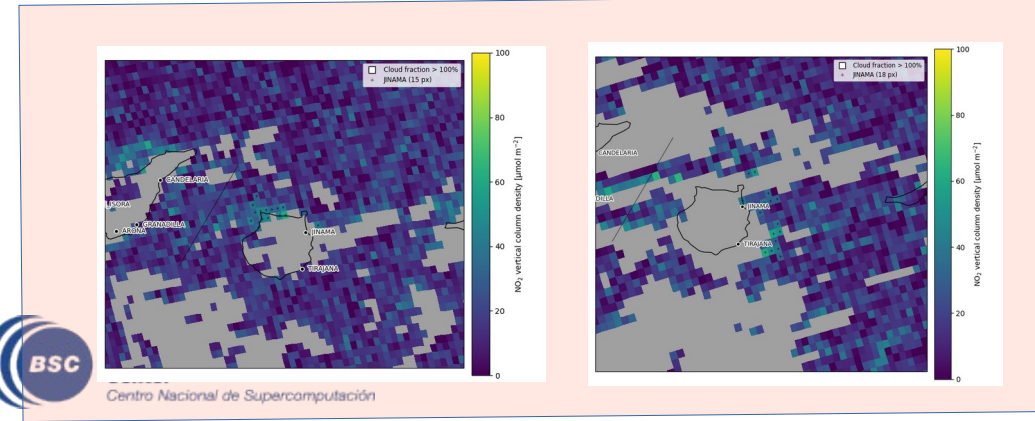
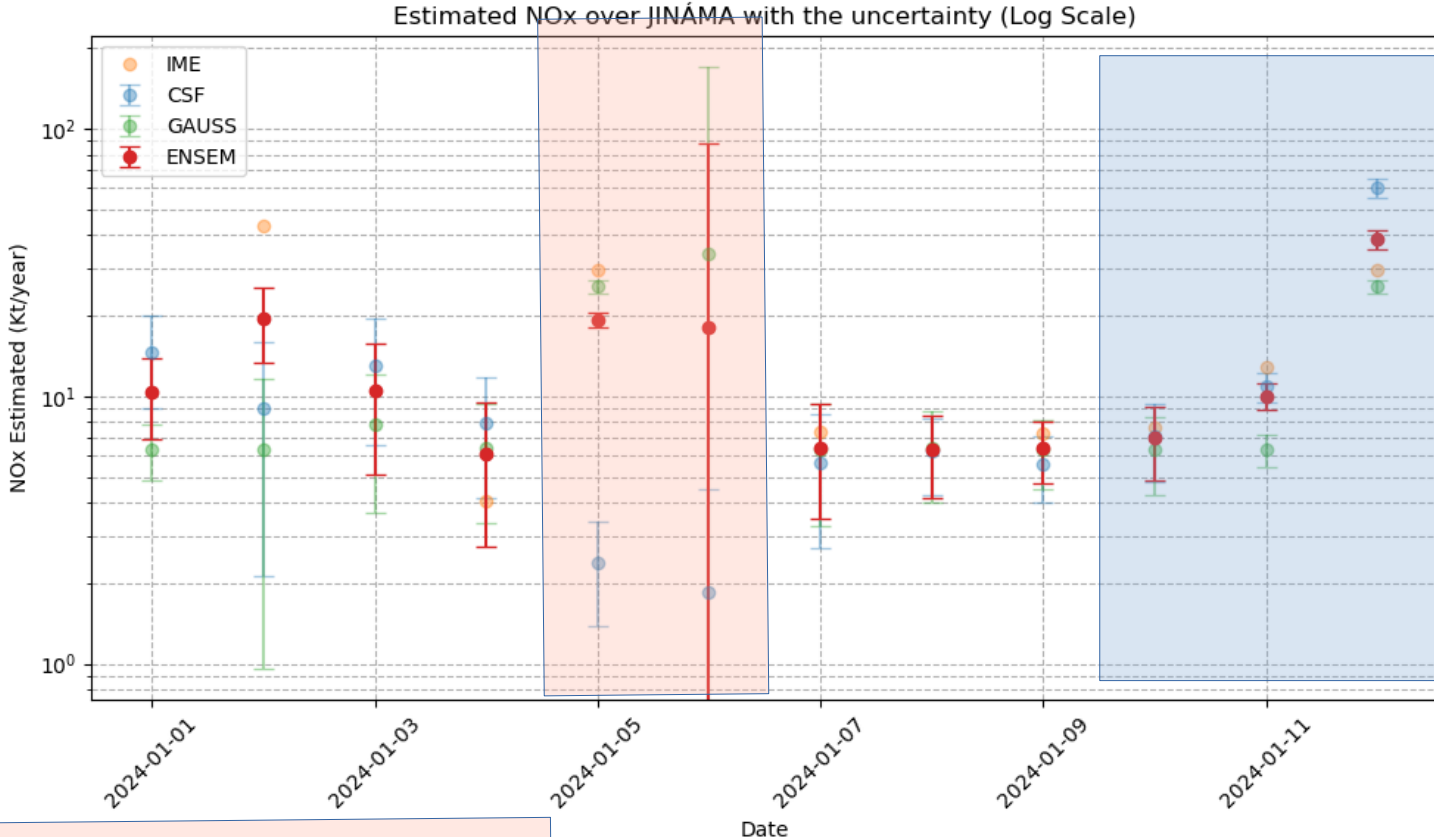
Light Cross Sectional Flux

$$Q_{NO_x} = f \cdot Q_{NO_2} \cdot \exp\left(-\frac{x}{u \times t}\right),$$

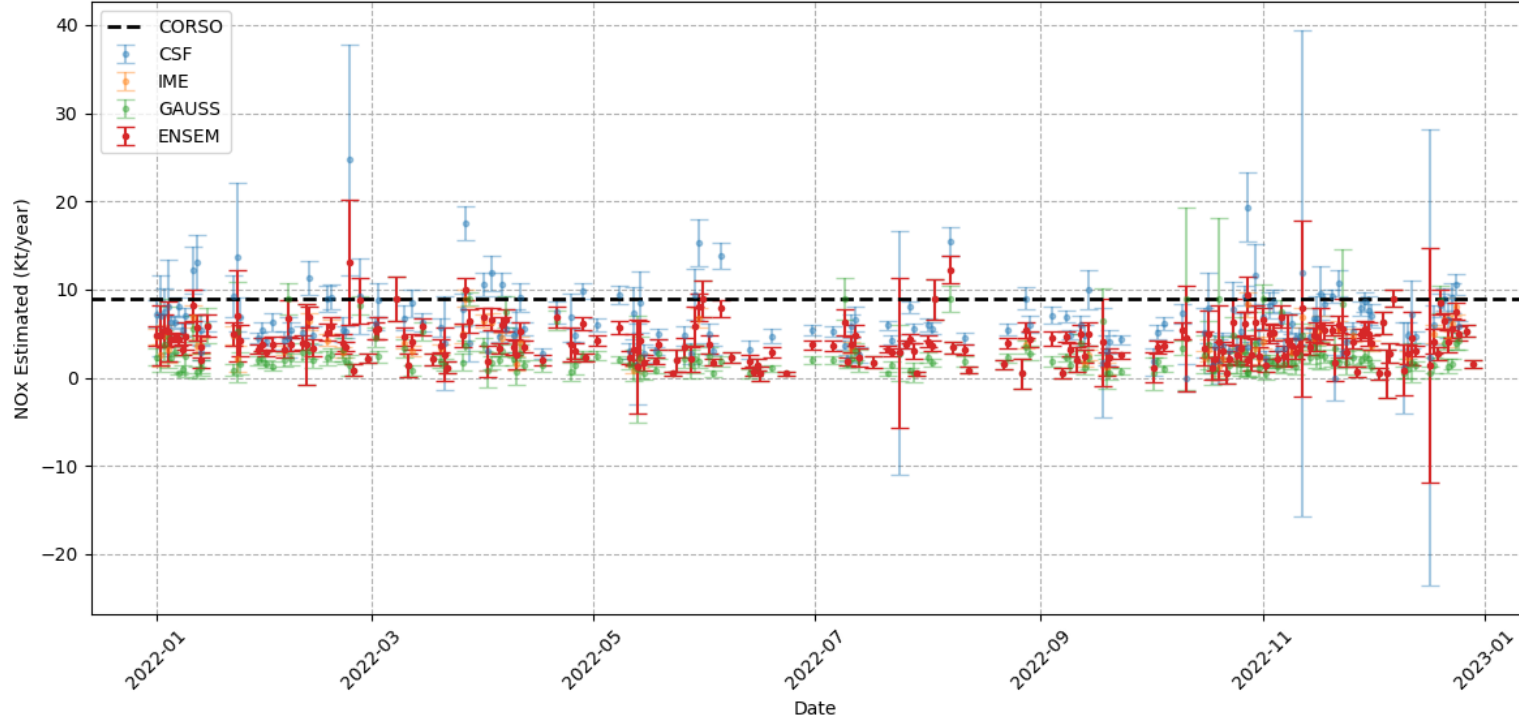


Each of these methods has its own uncertainty measure

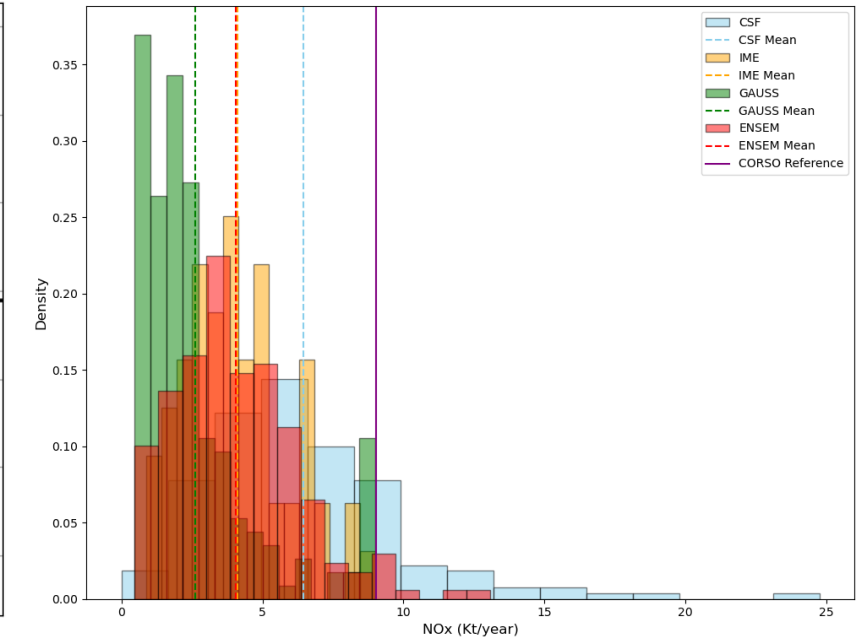
Lightweight emission estimation methods



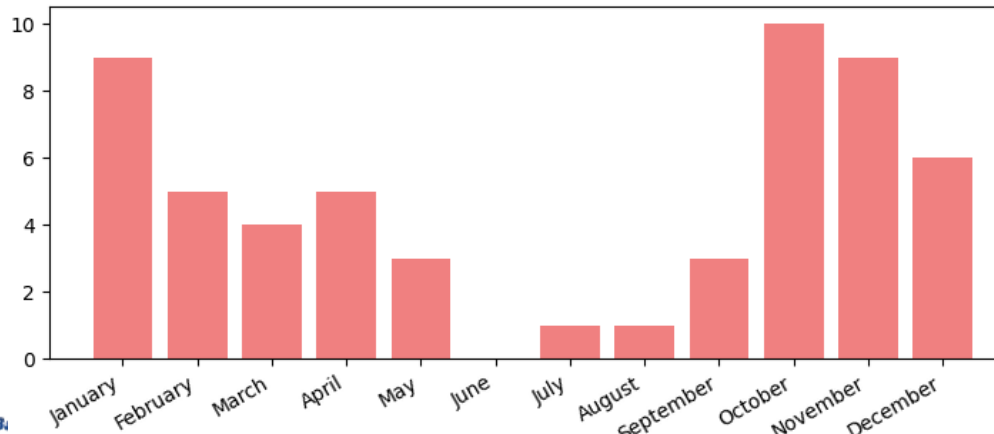
Estimated NOx over Punta Piedra (2022) with Uncertainty (Log Scale)



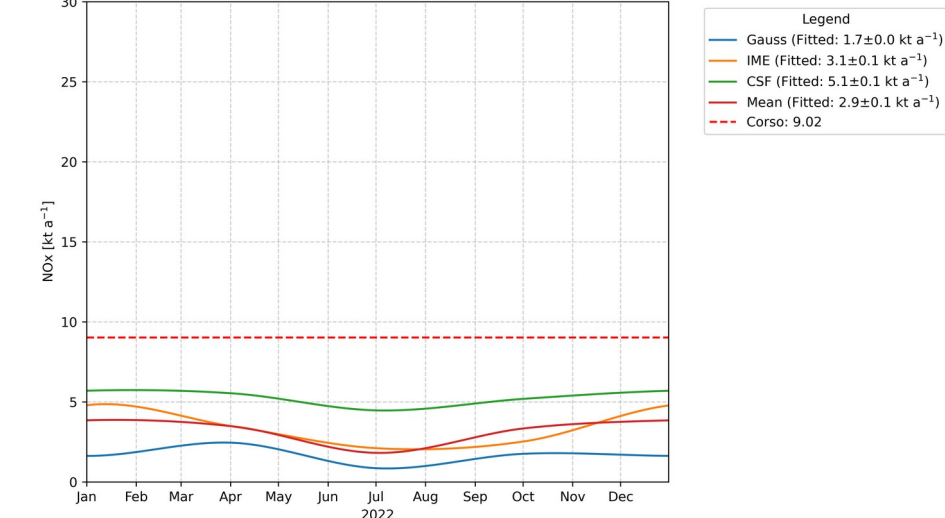
Distribution of NOx Estimates with Mean and CORSO Reference Lines



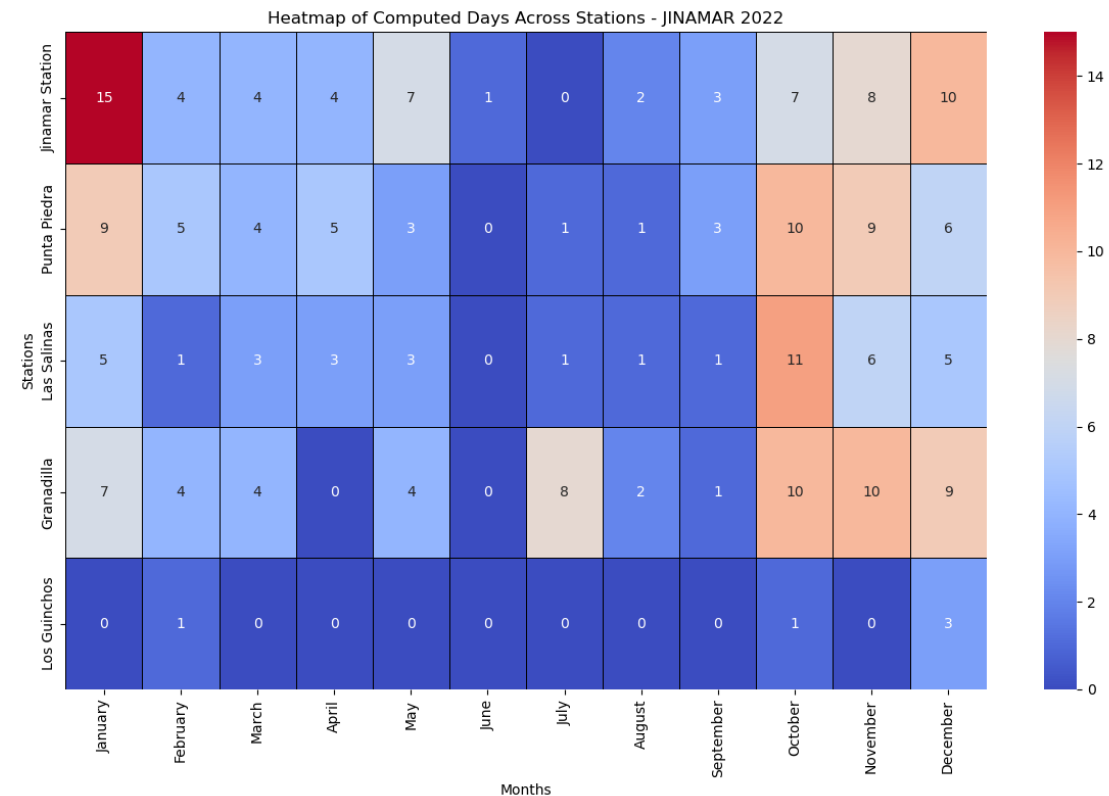
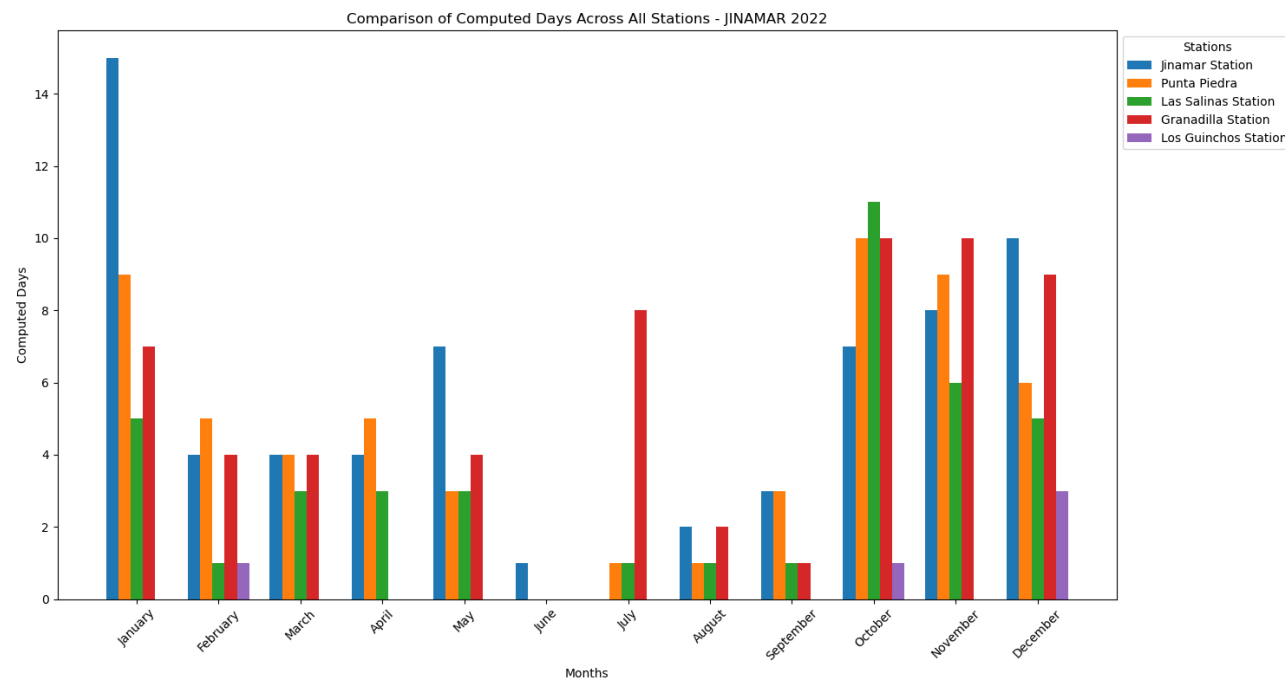
Power plant - Punta Piedra

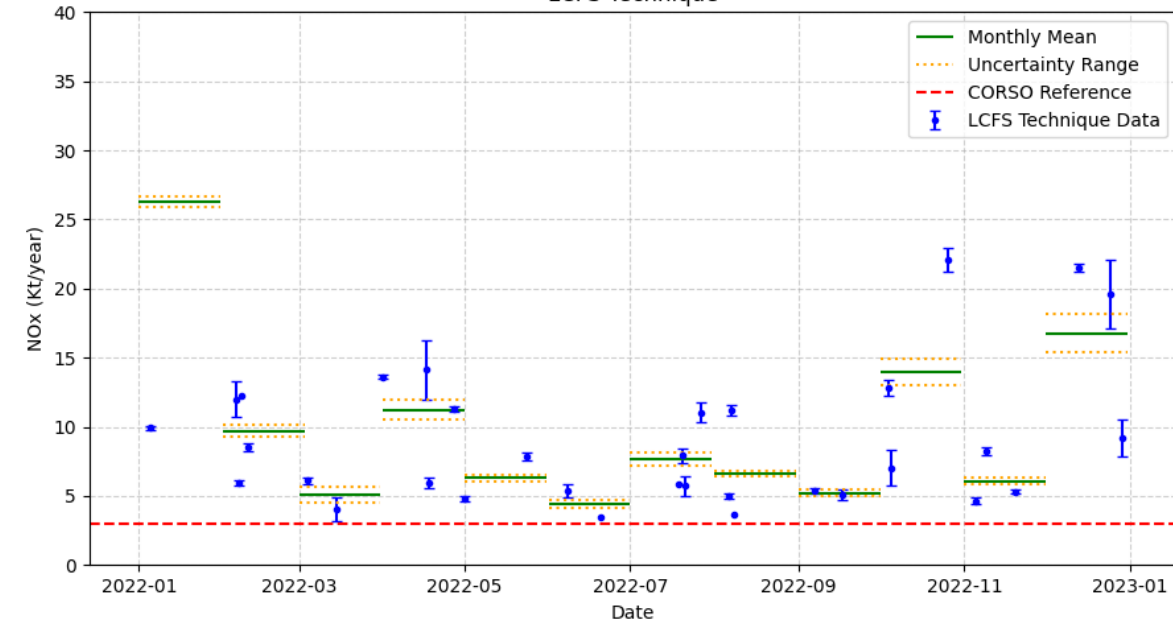
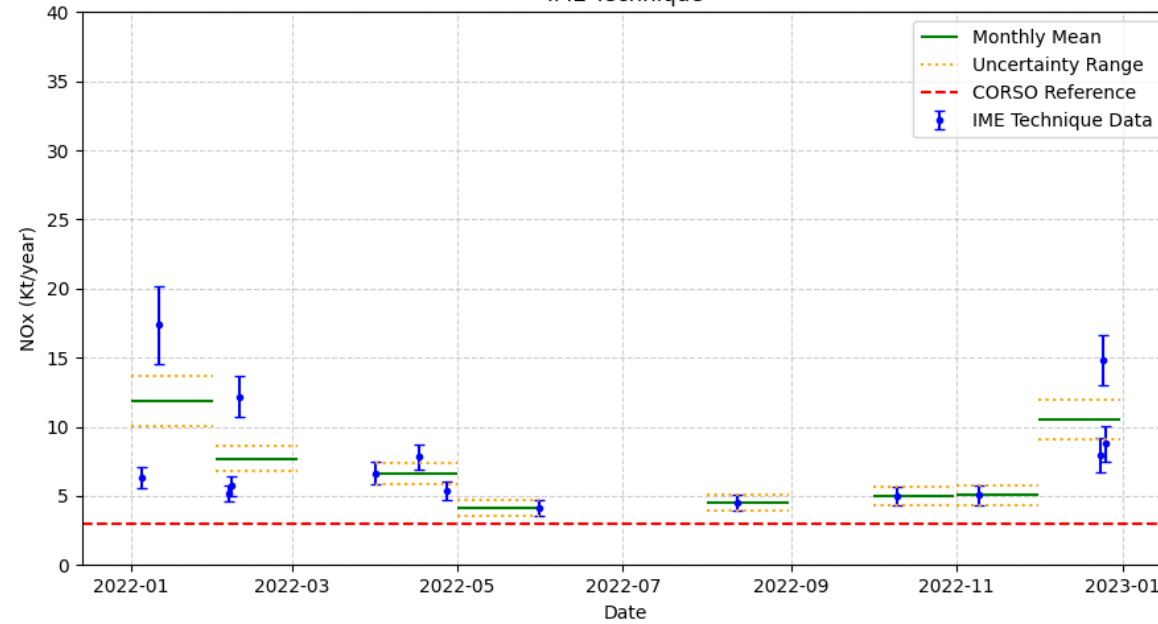
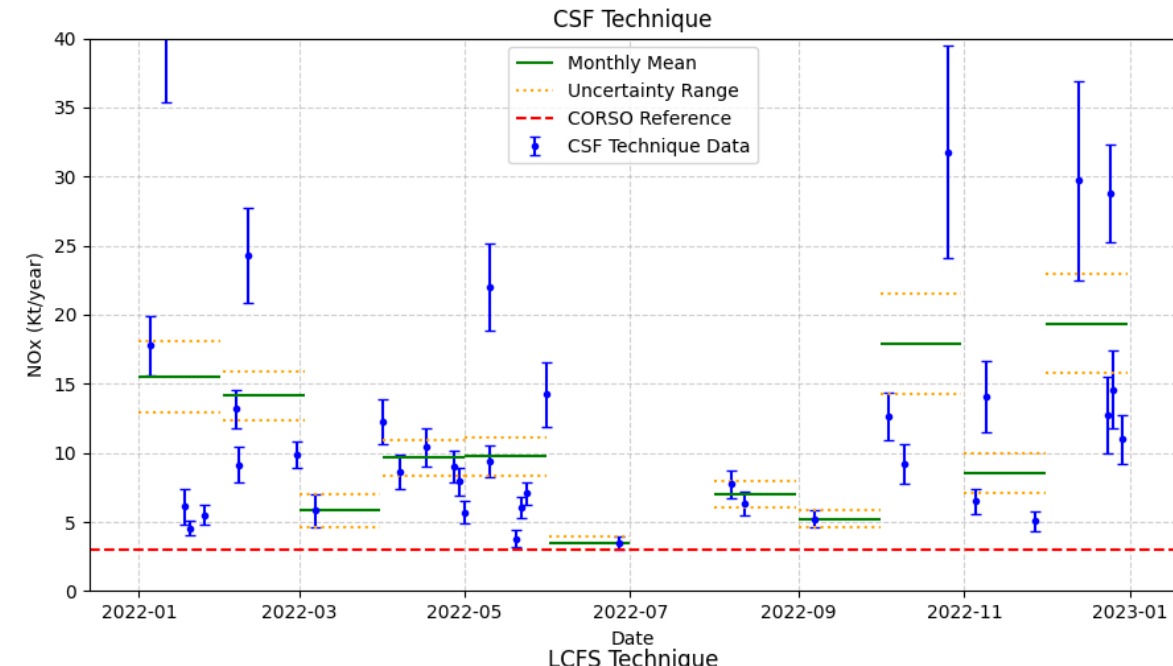
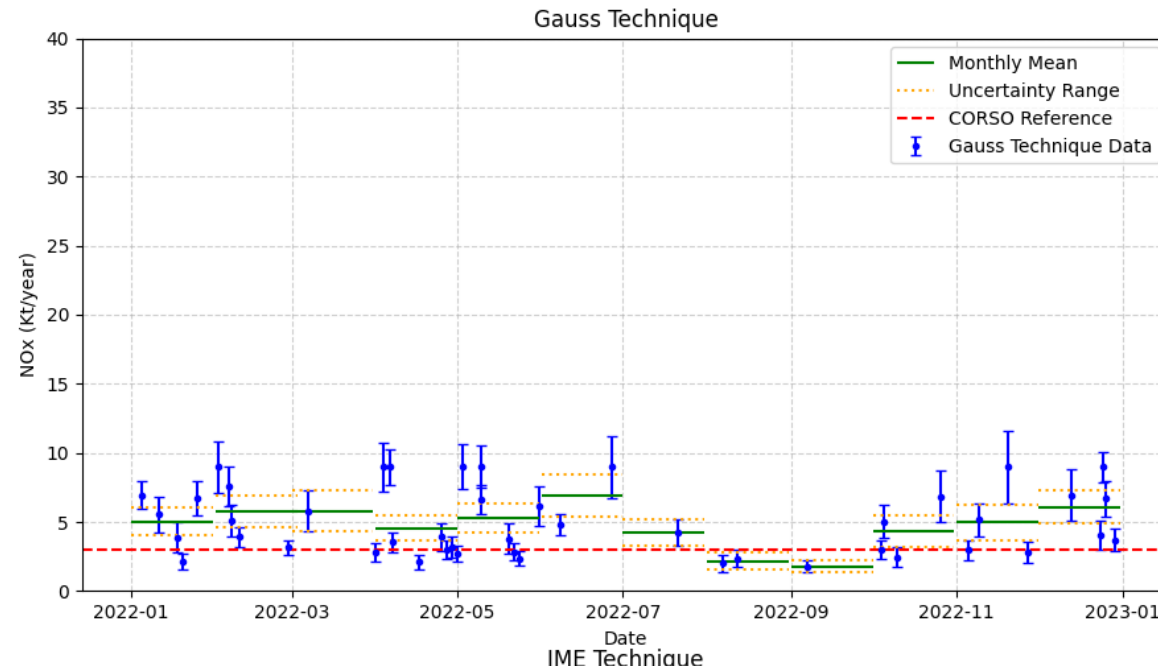


NOx Emissions for PUNTA_GRANDE



Available detections over one year over the Canary Islands





Early conclusions

- The pixel resolution of atmospheric composition satellites (i.e. orbital spectrometers) is known to be improving over time, yet remains comparatively coarse in comparison to satellites in the visible spectrum. Nevertheless, the advent of high spatio-temporal resolution from atmospheric composition will demand lightweight methods to generate real-time emission inventories.
- A positive correlated variability of the emitted values and the reference is observed for the Intermountain and New Madrid power plants emission estimated values compared with daily basis emissions reported.
- After filtering with the uncertainty flag based on the percentile the technique with the lower RMSE was the IME(**8.30**) and LCSF(**8.63**). The lower abs(MFB) correspond to the CSF(**14.4%**) and LCSF(**8.94**) The higher correlation correspond to the LCSF (**0.35**)
- Several aspects need to be revised in order to improve the emission estimation capability of the lightweight methods for satellite-based emission estimation (**NO_x/NO₂ conversion factor, NO₂ lifetime, Topography corrections, TROPOMI a priori profile, representativity of the winds**).
- It is crucial to conduct a stage per day of filter size determination in order to distinguish near plumes in non-isolated locations.
- Lightweight methods can estimate emissions on a daily basis, local time of passing (solar synchronous orbit) and hourly (geostationary orbit) which could be an independent validation tool of low latency emission inventories.



Funded by
the European Union



References

- [1] G. Leguizti et al. "Quantification of carbon monoxide emissions from African cities using TROPOMI". In: *Atmospheric Chemistry and Physics* 23 (2023), pp. 8899–8919. DOI: 10.5194/acp-23-8899-2023.
- [2] D. Santaren et al. "Benchmarking data-driven inversion methods for the estimation of local CO₂ emissions from XCO₂ and NO₂ satellite images". In: *Atmospheric Measurement Techniques Discussions [preprint]* (2024). DOI: 10.5194/amt-2023-241.
- [3] Gerrit Kuhlmann et al. "Quantifying CO₂ emissions of power plants with CO₂ and NO₂ imaging satellites". In: *Frontiers in Remote Sensing* 2 (2021), p. 689838.
- [4] Matthieu Pommier. "Estimations of NO_x emissions, NO₂ lifetime and their temporal variation over three British urbanised regions in 2019 using TROPOMI NO₂ observations". In: *Environmental Science: Atmospheres* 3.2 (2023), pp. 408–421.
- [5] H Bovensmann et al. "A remote sensing technique for global monitoring of power plant CO₂ emissions from space and related applications". In: *Atmospheric Measurement Techniques* 3.4 (2010), pp. 781–811.
- [6] John M Stockie. "The mathematics of atmospheric dispersion modeling". In: *Siam Review* 53.2 (2011), pp. 349–372.
- [7] Ray Nassar et al. "Quantifying CO₂ emissions from individual power plants from space". In: *Geophysical Research Letters* 44.19 (2017), pp. 10–045.
- [8] Ray Nassar et al. "Tracking CO₂ emission reductions from space: A case study at Europe's largest fossil fuel power plant". In: *Frontiers in Remote Sensing* 3 (2022), p. 1028240.
- [9] Thomas Lauvaux et al. "Global assessment of oil and gas methane ultra-emitters". In: *Science* 375.6580 (2022), pp. 557–561.
- [10] Erik Koene et al. *Documentation of plume detection and quantification methods*. Tech. rep. Technical Report 4.3, Empa, <https://www.coco2-project.eu/node/329>, 2021.
- [11] Stephen Conley et al. "Application of Gauss's theorem to quantify localized surface emissions from airborne measurements of wind and trace gases". In: *Atmospheric Measurement Techniques* 10.9 (2017), pp. 3345–3358.
- [12] Daniel J Varon et al. "Quantifying methane point sources from fine-scale satellite observations of atmospheric methane plumes". In: *Atmospheric Measurement Techniques* 11.10 (2018), pp. 5673–5686.
- [13] Gijs Leguizti et al. "Quantification of carbon monoxide emissions from African cities using TROPOMI". In: *Atmospheric Chemistry and Physics* 23.15 (2023), pp. 8899–8919.
- [14] Bo Zheng et al. "Observing carbon dioxide emissions over China's cities and industrial areas with the Orbiting Carbon Observatory-2". In: *Atmospheric Chemistry and Physics* 20.14 (2020), pp. 8501–8510.
- [15] Frédéric Chevallier et al. "Large CO₂ emitters as seen from satellite: comparison to a gridded global emission inventory". In: *Geophysical Research Letters* 49.5 (2022), e2021GL097540.
- [16] Steffen Beirle et al. "Pinpointing nitrogen oxide emissions from space". In: *Science advances* 5.11 (2019), eaax9800.
- [17] S Beirle et al. *Catalog of NO_x emissions from point sources as derived from the divergence of the NO₂ flux for TROPOMI*. Earth System Science Data Discussions [preprint], 2021, 1–28. 2021.
- [18] Janne Hakkarainen et al. "Analyzing local carbon dioxide and nitrogen oxide emissions from space using the divergence method: An application to the synthetic smartcarb dataset". In: *Frontiers in Remote Sensing* 3 (2022), p. 878731.
- [19] JP Veefkind et al. "Widespread frequent methane emissions from the oil and gas industry in the Permian basin". In: *Journal of Geophysical Research: Atmospheres* 128.3 (2023), e2022JD037479.
- [20] F. Cifuentes et al. "Accurate space-based NO_x emission estimates with the flux divergence approach require fine-scale model information on local oxidation chemistry and profile shapes". In: *EGUphere* 2024 (2024), pp. 1–40. DOI: 10.5194/egusphere-2024-2225. URL: <https://egusphere.copernicus.org/preprints/2024/egusphere-2024-2225/>.
- [21] Mengyao Liu et al. "Current potential of CH₄ emission estimates using TROPOMI in the Middle East". In: *Atmospheric Measurement Techniques* 17.17 (2024), pp. 5261–5277.
- [22] Xiaoxing Zuo et al. "Observing Downwind Structures of Urban HCHO Plumes From Space: Implications to Non-Methane Volatile Organic Compound Emissions". In: *Geophysical Research Letters* 50.24 (2023), e2023GL106062.
- [23] S. Beirle et al. "Improved catalog of NO_x point source emissions (version 2)". In: *Earth System Science Data* 15.7 (2023), pp. 3051–3073. DOI: 10.5194/essd-15-3051-2023. URL: <https://essd.copernicus.org/articles/15/3051/2023/>.
- [24] Christian Frankenberg et al. "Airborne methane remote measurements reveal heavy-tail flux distribution in Four Corners region". In: *Proceedings of the national academy of sciences* 113.35 (2016), pp. 9734–9739.
- [25] B. J. Schuit et al. "Automated detection and monitoring of methane super-emitters using satellite data". In: *Atmospheric Chemistry and Physics* 23.16 (2023), pp. 9071–9098. DOI: 10.5194/acp-23-9071-2023. URL: <https://acp.copernicus.org/articles/23/9071/2023/>.
- [26] Jack H Bruno et al. "U-Plume: automated algorithm for plume detection and source quantification by satellite point-source imagers". In: *Atmospheric Measurement Techniques* 17.9 (2024), pp. 2625–2636.
- [27] S. Meier et al. "A light-weight NO₂ to NO_x conversion model for quantifying NO_x emissions of point sources from NO₂ satellite observations". In: *EGUphere* [preprint] (2024). DOI: 10.5194/egusphere-2024-159.
- [28] Maarten Krol et al. "Evaluating NO_x stack plume emissions using a high-resolution atmospheric chemistry model and satellite-derived NO₂ columns". In: *Atmospheric Chemistry and Physics* 24.14 (2024), pp. 8243–8262.
- [29] G. Kuhlmann et al. "The ddeq Python library for point source quantification from remote sensing images (version 1.0)". In: *Geoscientific Model Development* 17.12 (2024), pp. 4773–4789. DOI: 10.5194/gmd-17-4773-2024.
- [30] Gerrit Kuhlmann et al. "Mapping the spatial distribution of NO₂ with in situ and remote sensing instruments during the Munich NO₂ imaging campaign". In: *Atmospheric Measurement Techniques* 15.6 (2022), pp. 1609–1629.
- [31] E. F. M. Koene, D. Brunner, and G. Kuhlmann. "On the theory of the divergence method for quantifying source emissions from satellite observations". In: *Journal of Geophysical Research: Atmospheres* 129.12 (2024), e2023JD039904. DOI: 10.1029/2023JD039904.
- [32] Janne Hakkarainen et al. "Analyzing nitrogen dioxide to nitrogen oxide scaling factors for data-driven satellite-based emission estimation methods: A case study of Matimba/Medupi power stations in South Africa". In: *Atmospheric Pollution Research* 15.7 (2024), p. 102171.
- [33] Xiaojuan Lin et al. "Monitoring and quantifying CO₂ emissions of isolated power plants from space". In: *Atmospheric Chemistry and Physics* 23.11 (2023), pp. 6599–6611.
- [34] Sandro Meier et al. "A lightweight NO₂-to-NO_x conversion model for quantifying NO_x emissions of point sources from NO₂ satellite observations". In: *Atmospheric Chemistry and Physics* 24.13 (2024), pp. 7667–7686.
- [35] Daniel L Goldberg et al. "Enhanced capabilities of TROPOMI NO₂: Estimating NO_X from north american cities and power plants". In: *Environmental science & technology* 53.21 (2019), pp. 12594–12601.
- [36] Alexandre Danjou et al. "Evaluation of light atmospheric plume inversion methods using synthetic XCO₂ satellite images to compute Paris CO₂ emissions". In: *Remote Sensing of Environment* 305 (2024), p. 113900.
- [37] Anthony Rey-Pommier et al. "Mapping NO_x emissions in Cyprus using TROPOMI observations: evaluation of the flux-divergence scheme using multiple parameter sets". In: *Environmental Science and Pollution Research* (2025), pp. 1–20.
- [38] M. Guevara et al. *CoCO2 global emission point source database*. Dataset. Accessed: 2024-07-25. Mar. 2023. URL: <https://atmosphere.copernicus.eu/node/865>.
- [39] Tao Tang et al. "Quantifying instantaneous nitrogen oxides emissions from power plants based on space observations". In: *Science of The Total Environment* 938 (2024), p. 173479.
- [40] Gerrit Kuhlmann et al. "Detectability of CO₂ emission plumes of cities and power plants with the Copernicus Anthropogenic CO₂ Monitoring (CO2M) mission". In: *Atmospheric Measurement Techniques* 12.12 (2019), pp. 6695–6719.
- [41] J Pepijn Veefkind et al. "TROPOMI on the ESA Sentinel-5 Precursor: A GMES mission for global observations of the atmospheric composition for climate, air quality and ozone layer applications". In: *Remote sensing of environment* 120 (2012), pp. 70–83.
- [42] JHGM Van Geffen et al. "TROPOMI ATBD of the total and tropospheric NO₂ data products". In: *DLR document* (2019).
- [43] Daniel A Potts et al. "Identifying and accounting for the Coriolis effect in satellite NO₂ observations and emission estimates". In: *Atmospheric Chemistry and Physics* 23.7 (2023), pp. 4577–4593.
- [44] KF Boersma et al. "An improved tropospheric NO₂ column retrieval algorithm for the Ozone Monitoring Instrument". In: *Atmospheric Measurement Techniques* 4.9 (2011), pp. 1905–1928. DOI: <https://doi.org/10.5194/amt-4-1905-2011>.
- [45] Hans Hersbach et al. "The ERA5 global reanalysis". In: *Quarterly Journal of the Royal Meteorological Society* 146.730 (2020), pp. 1999–2049.
- [46] H. Hersbach et al. *ERA5 hourly data on pressure levels from 1940 to present*. Accessed on DD-MMM-YYYY. 2023. DOI: 10.24381/cds.b0915c6.
- [47] E. Dammers et al. "Can TROPOMI-NO₂ satellite data be used to track the drop and resurgence of NO_x emissions between 2019–2021 using the multi-source plume method (MSPM)?". In: *Geoscientific Model Development Discussions* (2022), pp. 1–33.

Questions